



# Kinetics of hydroformylation of 1-octene in ionic liquid-organic biphasic media using rhodium sulfoxantphos catalyst

Raj M. Deshpande, Ashutosh A. Kelkar, Amit Sharma, Carine Julcour-Lebigue, Henri Delmas

## ► To cite this version:

Raj M. Deshpande, Ashutosh A. Kelkar, Amit Sharma, Carine Julcour-Lebigue, Henri Delmas. Kinetics of hydroformylation of 1-octene in ionic liquid-organic biphasic media using rhodium sulfoxantphos catalyst. Chemical Engineering Science, 2011, vol. 66 (n° 8), pp. 1631-1639. 10.1016/J.CES.2010.12.040 . hal-03539045

**HAL Id: hal-03539045**

**<https://hal.science/hal-03539045>**

Submitted on 21 Jan 2022

**HAL** is a multi-disciplinary open access archive for the deposit and dissemination of scientific research documents, whether they are published or not. The documents may come from teaching and research institutions in France or abroad, or from public or private research centers.

L'archive ouverte pluridisciplinaire **HAL**, est destinée au dépôt et à la diffusion de documents scientifiques de niveau recherche, publiés ou non, émanant des établissements d'enseignement et de recherche français ou étrangers, des laboratoires publics ou privés.



## Open Archive Toulouse Archive Ouverte (OATAO)

OATAO is an open access repository that collects the work of Toulouse researchers and makes it freely available over the web where possible.

This is an author-deposited version published in: <http://oatao.univ-toulouse.fr/>  
Eprints ID: 6179

**To link to this article:** DOI:10.1016/J.CES.2010.12.040  
URL: <http://dx.doi.org/10.1016/J.CES.2010.12.040>

**To cite this version:** Deshpande, Raj M. and Kelkar, Ashutosh A. and Sharma, Amit and Julcour-Lebigue, Carine and Delmas, Henri (2011) Kinetics of hydroformylation of 1-octene in ionic liquid-organic biphasic media using rhodium sulfoxantphos catalyst. *Chemical Engineering Science*, vol. 66 (n°8). pp. 1631-1639. ISSN 0009-2509

Any correspondence concerning this service should be sent to the repository administrator: [staff-oatao@listes.diff.inp-toulouse.fr](mailto:staff-oatao@listes.diff.inp-toulouse.fr)

# Kinetics of hydroformylation of 1-octene in ionic liquid-organic biphasic media using rhodium sulfoxantphos catalyst

R.M. Deshpande<sup>a</sup>, A.A. Kelkar<sup>a</sup>, A. Sharma<sup>b</sup>, C. Julcour-Lebigue<sup>b,\*</sup>, H. Delmas<sup>b</sup>

<sup>a</sup> Chemical Engineering Division, National Chemical Laboratory, Pune 411008, India

<sup>b</sup> Université de Toulouse, Laboratoire de Génie Chimique, UMR 5503 CNRS/ENSIACET, Toulouse, France

## A B S T R A C T

Biphasic hydroformylation of 1-octene was performed using rhodium sulfoxantphos catalyst dissolved in [BuPy][BF<sub>4</sub>] ionic liquid. Preliminary experiments proved this system to retain the catalytic complex within the ionic liquid phase and to maintain a high selectivity towards the linear aldehyde (*n*:iso ratio of 30) over several cycles. Process parameter investigation showed a first order dependence of the initial rate with respect to the catalyst and 1-octene concentrations, but a more complex behavior with respect to hydrogen (fractional order) and carbon monoxide partial pressures (inhibition at high pressures). Different mathematical models were selected based on the trends observed and evaluated for data fitting. Also, rate models were derived from a proposed mechanism, using Christiansen matrix approach. To calculate concentrations of substrates in the catalytic phase as required by this kinetic modeling, solubility measurements were performed for the gases (pressure drop technique), as well as for 1-octene and *n*-nonanal (thermogravimetry analysis).

## 1. Introduction

Hydroformylation of olefins is an important well-known process for the production of aldehydes and alcohols; moreover it is one of the most important applications of homogeneous catalysis in industry as well. In commercial processes, which use pure olefin as feedstock, values of TurnOver Frequency typically range 200–4000 mol<sub>aldehyde</sub>/mol<sub>metal</sub>/h for Rh-based catalysts (Beller et al., 1995; Arnoldy, 2000). However, difficulties in the separation of catalyst from the product and catalyst recycle have limited the application of this reaction on an industrial scale. Aqueous phase biphasic catalytic systems have opened a new perspective for transition metal complex driven homogeneous catalysis after the industrial success of propylene hydroformylation catalyzed by water-soluble HRh(CO)(TPPTS)<sub>3</sub> and developed by Rhone-Poulenc and RuhrChemie (Kuntz, 1987). Low solubility of higher olefins has limited the scope of water-soluble catalyst for the hydroformylation reaction. In order to overcome this difficulty, various new concepts like fluorous biphasic catalysis (Horvath and Rabai, 1994; Horvath and Rabai, 1995; Mathivet et al., 2002) and ionic liquid biphasic catalysis (Chauvin and Olivier-Bourbigou, 1995; Welton, 1999; Zhao et al., 2002; Haumann and Riisager, 2008) have been investigated

and ionic liquids have successfully been applied as alternative solvents for homogeneous catalysis.

Non Aqueous Ionic Liquids [NAILs] are ionic media, comprising of ionic compounds which are liquid at room temperature or at an operating reaction temperature. They are good solvents for a wide range of both organic and inorganic materials. Also, their solubility and acidity/coordination properties can be tuned by varying the nature of the anion and cation systematically. The possibility of adjusting solubility properties is of an importance for liquid–liquid biphasic catalysis. These unique properties have made them ideal for use as solvents in homogeneous catalysis (Chauvin and Olivier-Bourbigou, 1995; Welton, 1999; Zhao et al., 2002).

Hydroformylation in NAILs-organic biphasic media has been investigated by a number of researchers. The first report on the rhodium catalyzed hydroformylation using an ionic liquid was proposed by Chauvin et al. (1995). However, use of triphenyl phosphine as a ligand led to significant leaching of rhodium catalyst. Use of TPPMS (diphenyl(3-sulfonatophenyl) phosphane monosodium salt) reduced the extent of rhodium leaching. Polar ligands such as TPPTS (tris(3-sulfonatophenyl) phosphane trisodium salt) were used to modify the Rh precursor (Rh(CO)<sub>2</sub>(acac)) and an easy catalyst/product separation was reported (Kong et al., 2004). Various ligands have been used for ionic liquid biphasic system for the hydroformylation of olefins (Brasse et al., 2000; Favre et al., 2001; Kottsieper et al., 2001; Brauer et al., 2001; Wasserscheid et al., 2001, 2002; Kong et al., 2004; Omotowa and Shreeve, 2004; Mehnert et al., 2004; Deng et al., 2007; Peng et al., 2007). Dupont et al. (2001)

\* Corresponding author. Tel.: +33 534323709; fax: +33 534323697.

E-mail addresses: raj.m.deshpande@gmail.com (R.M. Deshpande), carine.julcour@ensiacet.fr (C. Julcour-Lebigue).

have investigated hydroformylation of higher olefins in an ionic liquid using sulfoxantphos as ligand and  $\text{Rh}(\text{CO})_2(\text{acac})$  as the catalyst precursor. They observed that the selectivity is strongly influenced by the nature of the ionic liquid. The highest *n*:iso ratio of 61 was obtained with 79% conversion of 1-octene using  $[\text{Bmim}][\text{PF}_6]$  ionic liquid at 100 °C and 24 h reaction time. However, there are no detailed reports on the hydroformylation of higher olefins using Rh-sulfoxantphos catalyst system and ionic liquid biphasic system. Also, there are very few studies on the kinetics of hydroformylation of olefins in such biphasic media (Sharma et al., 2010). Since NAILs possess many properties which could lend itself to coordination of the metal complex/center, it would be of interest to investigate the role of different process parameters on the activity and selectivity of the catalyst. We report here the detailed kinetics of the hydroformylation of 1-octene using a water-soluble Rh-sulfoxantphos catalyst, in a two-phase system, comprising of  $[\text{BuPy}][\text{BF}_4]$  ionic liquid as the catalyst phase and heptane as the organic phase. The study has been carried out in a temperature range 353–373 K. Rate equations have been proposed and kinetic parameters have been estimated.

## 2. Experimental

### 2.1. Materials

$\text{RhCl}_3 \cdot 3\text{H}_2\text{O}$  (Arora Matthey, India), xantphos,  $\text{P}_2\text{O}_5$ , trioctyl amine (Aldrich, USA),  $\text{H}_2\text{SO}_4$  (Loba Chemicals, India), pyridine,  $\text{NaBF}_4$  (Aldrich, USA),  $\text{NaOH}$  (Loba Chemicals, India), heptane, 1-octene, *n*-nonanal (Aldrich, USA), bromobutane and methanol (Loba Chemicals, India) were used as received.  $\text{Rh}(\text{CO})_2(\text{acac})$  and sulfoxantphos were prepared as per the literature procedures (Varshavskii and Cherkasova, 1967; Goedheijt et al., 1998). Hydrogen (Indian Oxygen, Bombay) and carbon monoxide (> 99.8% pure, Matheson Gas, USA) were used directly from cylinders. The syngas mixture ( $[\text{H}_2 + \text{CO}]$  with 1:1 ratio) was prepared by mixing  $\text{H}_2$  and CO in a reservoir vessel.  $[\text{BuPy}][\text{Br}]$  was prepared using the literature procedure (Owens and Abu-Omar, 2002) and the ionic liquid *n*-butylpyridinium tetrafluoroborate was synthesized using a cation exchange resin. An ICP analysis of resulting IL showed very little bromide content, in the range 35–45 ppm.

### 2.2. Experimental set-up

All the hydroformylation experiments were carried out in a 50 ml reactor, made of stainless steel and supplied by Amar Instruments India Pvt. Ltd. The reactor was provided with liquid and gas sampling devices, automatic temperature control and variable agitation speed. It was designed for a working pressure of 210 bar and temperature up to 523 K. The consumption of CO and  $\text{H}_2$  at a constant pressure was monitored by observing, as a function of time, the pressure drop in the gas reservoir from which the equimolar ( $\text{CO} + \text{H}_2$ ) mixture was supplied.

### 2.3. Experimental procedure for catalytic hydroformylation

The rhodium sulfoxantphos catalyst precursor was prepared as per the procedure described by Goedheijt et al. (1998). In a typical experiment, sulfoxantphos and  $\text{Rh}(\text{CO})_2(\text{acac})$  were mixed in the desired ratio, in 10 ml of degassed  $[\text{BuPy}][\text{BF}_4]$  under an argon atmosphere. The resulting yellowish solution was transferred into the autoclave. The autoclave was then flushed three times with nitrogen and syngas respectively, pressurized to 13.6 bar with  $\text{CO}/\text{H}_2$  and heated to 393 K under stirring for 12 h. Thereafter, the reactor was cooled to 298 K and depressurized. A light yellow colored solution of the catalyst was formed. The reactor was then

loaded with the olefin and heptane (15 ml) as the organic phase for the reaction. The contents were flushed with nitrogen, and then with a mixture of CO and  $\text{H}_2$  and heated to attain the desired temperature (353, 363 or 373 K). Afterwards a mixture of CO and  $\text{H}_2$  (in a required ratio, 1:1) was introduced into the autoclave up to the desired pressure (41.4 bar under standard conditions). A sample of the organic phase was withdrawn, and the reaction started by switching the stirrer on. The reaction was then carried out at a constant pressure of  $\text{CO} + \text{H}_2$  (1:1) by the supply of syngas from the reservoir vessel through a constant pressure regulator. Since, in this study, the major product formed was an aldehyde, supply of  $\text{CO} + \text{H}_2$  at a ratio of 1:1 (as per stoichiometry) was adequate to maintain a constant composition of  $\text{H}_2$  and CO in the reactor, as introduced in the beginning. After the completion of reaction, the reactor was cooled and a final sample was taken for analysis. In each kinetic run, organic phase samples were withdrawn at specific time intervals and analyzed for reactants and products in order to check the progress of the reaction and material balance. In a few experiments, gas consumption was monitored and found to match with the amount of liquid products formed as per the stoichiometry of the reaction. Thus, no gaseous by-products were formed during the reaction. It was generally observed that in this low conversion range (< 15% in most cases), the rates of hydroformylation were constant. The reproducibility of the experiments was found to be in a range 5–7%. Following this procedure, the effect of the catalyst and olefin concentrations, partial pressures of  $\text{H}_2$  and CO, and temperature on the rate of hydroformylation was studied.

### 2.4. Analytical methods

Organic phase samples were analyzed on a HP-5 capillary column (30 m  $\times$  320  $\mu\text{m}$   $\times$  0.25  $\mu\text{m}$  film thickness with a stationary phase of 5% phenyl-methyl siloxane), using a Hewlett Packard 6890 Series GC controlled by HP Chemstation software and equipped with an auto sampler unit. The quantitative analysis was carried out using an external standard method by constructing a calibration-table for reactants and products in the range of concentrations studied.

## 3. Results and discussion

### 3.1. Solubility data

As the knowledge of the reactant concentrations in the ionic liquid (IL) phase is required for the interpretation and modeling of the kinetic data, the solubility of CO and  $\text{H}_2$  in  $[\text{BuPy}][\text{BF}_4]$  was measured by the pressure variation method. Also, solubility of 1-octene and product *n*-nonanal in  $[\text{BuPy}][\text{BF}_4]$  was measured by the thermogravimetry analysis.

#### 3.1.1. Solubility of gaseous substrates in $[\text{BuPy}][\text{BF}_4]$

Gas solubility experiments were carried out in a 300  $\text{cm}^3$  capacity autoclave reactor (Hastelloy C276), equipped with a gas inducing impeller. Before performing the solubility experiments, free volume of the reactor was determined by filling it with nitrogen from a reservoir of known volume and measuring the pressure variation. The free volume of the reactor was found to be  $289 \pm 1$  ml, after three consecutive measurements at various initial pressures. Experiments for both  $\text{CO}-[\text{BuPy}][\text{BF}_4]$  and  $\text{H}_2-[\text{BuPy}][\text{BF}_4]$  systems were performed with a liquid volume of 85  $\text{cm}^3$  at three different temperatures: 333, 353 and 373 K. The temperature of the liquid was controlled within  $\pm 1$  K.

In a typical experiment, the reactor was filled with a known amount of ionic liquid and heated to the desired temperature. After the temperature was equilibrated, the ionic liquid was saturated with

the studied gas at low pressure ( $P_{atm}$ ), using high stirring rate (1200 rpm) for about 15 min. Then, the stirring was stopped and the gas solute pressure was rapidly increased in the reactor. The liquid was stirred again at 1200 rpm to reach a new equilibrium with the gas phase. The change in pressure was recorded online as a function of time, using a high precision pressure sensor. From initial and final pressure readings, the molar concentration of the gaseous solute in the ionic liquid was calculated and Henry's constant ( $H$ ) was determined from the plot of equilibrium pressure as a function of the corresponding solute concentration. Henry's constants for CO and  $H_2$  in [BuPy][BF<sub>4</sub>] at the three temperatures are given in Table 1. The plot of  $\ln(H)$  as a function of  $1/T$  (Fig. 1) was then used to calculate the concentrations of CO and  $H_2$  in [BuPy][BF<sub>4</sub>] at the three reaction temperatures. A decrease in solubility of both CO and  $H_2$  was observed with an increasing temperature. For  $H_2$ , the plot of  $\ln(H)$  as a function of  $1/T$  does not show the linear trend. Similar behavior for the two gases has been also reported in the case of [Bmim][PF<sub>6</sub>] ionic liquid (Sharma et al., 2009).

### 3.1.2. Solubility of liquid substrates in [BuPy][BF<sub>4</sub>]

Liquid–liquid equilibrium study was carried out to determine the solubility of 1-octene (reactant) and *n*-nonanal (product) in an ionic liquid phase ([BuPy][BF<sub>4</sub>]). These data were further used to calculate the concentration of 1-octene in an IL phase and the total number of moles of aldehyde formed during the reaction (partitioned between organic and IL phases) from the GC analysis of the organic phase only. The technique employed for measuring the liquid–liquid equilibria was the classical shake flask method. An emulsion consisting of 10 ml IL and 15 ml organic substrate was kept overnight under stirring at the desired temperature. Later the biphasic mixture was separated in a jacketed settler (kept at the same equilibrium temperature). After 1 h, the denser ionic liquid phase was withdrawn and analyzed immediately by the thermogravimetry analysis. Analyses were performed by heating the sample at 423 K under an inert atmosphere (nitrogen) and recording the weight loss till no more variation was observed. ILs being reported to have non-measurable vapor pressure, the weight loss recorded by TGA corresponds to some IL impurities

**Table 1**  
Henry's constants ( $H$ ) for  $H_2$  and CO in [BuPy][BF<sub>4</sub>].

$T$ (K)	$H_{H_2}$ (bar $m_{IL}^3/kmol$ )	$H_{CO}$ (bar $m_{IL}^3/kmol$ )
333	470.3	419.3
353	507.0	454.8
373	723.6	486.8

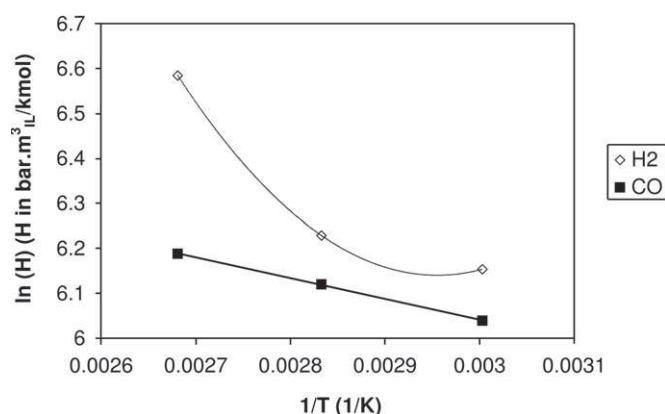


**Fig. 1.** Plot of  $\ln H$  (Henry's constant) versus the inverse of temperature.

**Table 2**

Partition coefficients ( $K_w$ ) of *n*-nonanal and 1-octene in [BuPy][BF<sub>4</sub>]. ( $K_w$  is given as the weight percentage of the solute in the IL phase to its weight percentage in the organic phase at equilibrium.)

$T$ (K)	$K_{w,non}$	$K_{w,oct}$
353	0.042	0.0036
363	0.045	0.0038
373	0.048	0.0041

and dissolved solute. Thus, prior to the analysis of the saturated sample, a blank measurement was performed on the ionic liquid itself (same lot) to quantify the amount of volatile impurities. This amount was subtracted from the total weight loss recorded with the saturated IL, assuming thus that the impurities were not transferred to the organic phase.

Further for the calculation of solute concentrations in the IL phase at the reaction conditions, it was assumed that heptane (and either octene or nonanal at low conversion range) did not modify the partition coefficient of either *n*-nonanal or 1-octene in the IL phase. This was checked on a similar system ([Bmim][PF<sub>6</sub>]-decane) by measuring with multiple headspace GC–MS, the partition coefficients of the two organic substrates for different mixtures of octene, nonanal and decane (Sharma et al., 2010). The partition coefficients obtained for 1-octene and *n*-nonanal are displayed in Table 2. As expected, the solubility of *n*-nonanal in [BuPy][BF<sub>4</sub>] is much higher than that of 1-octene, due to its higher polarity.

Based on these results, the initial concentrations of 1-octene in the IL phase were calculated and the initial rates of the reaction corrected to account for the amount of aldehyde solubilised in the IL phase.

### 3.2. Preliminary hydroformylation experiments

Choice of the solvent is important for the biphasic catalysis. Rh-sulfoxantphos catalyst is not soluble in alkane solvents, neither are usual ionic liquids. For these reasons, hexane, heptane, decane, etc. are good solvents for ionic liquid biphasic hydroformylation reactions. Heptane was chosen as a solvent for the reaction and preliminary experiments were conducted using [BuPy][BF<sub>4</sub>] (10 ml) as the catalyst phase and mixture of 1-octene and heptane (15 ml) as the organic phase.

The catalyst was synthesized *in situ* as per the procedure described in the experimental section and the hydroformylation of 1-octene was investigated at a syngas pressure of 41.4 bar and a temperature of 373 K. Other conditions were: P:Rh ratio of 10 and Rh loading of  $3.86 \times 10^{-3}$  kmol/ $m_{IL}^3$ . From the preliminary experiments, it was observed that the mass balance considering the substrates reacted and products formed were in good agreement (~95%). An *n*:iso ratio of 30 was observed, which also confirmed the formation of the Rh-sulfoxantphos catalytic complex. High selectivity to the linear aldehyde is indeed attributed to the favorable bite angle of the bidentate ligand used. Isomerization of 1-octene was observed as a side reaction, resulting in the formation of branched products (3–4% of the total aldehyde).

Leaching of the rhodium complex is a major problem in the ionic liquid biphasic catalyst system. In order to confirm that the rhodium leaching was not taking place and the catalyst present in the [BuPy][BF<sub>4</sub>] phase was still active after the reaction, recycle experiments were carried out under same conditions as described previously, excepting temperature of 393 K. At the end of the reaction (6 h), the autoclave was cooled to room temperature and allowed to stand for some time. The reactor was opened, the organic layer was separated quickly and a fresh charge of heptane and 1-octene was added to the reactor. The reactor was closed quickly and flushed 3–4 times with syngas mixture to remove



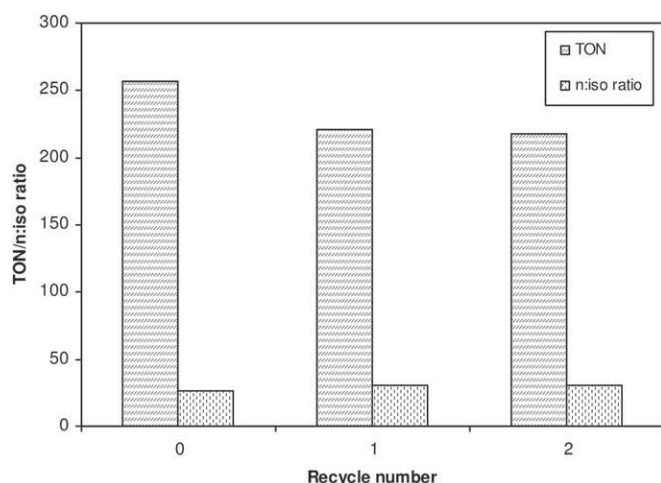


**Fig. 2.** Catalyst recycle experiment. Reaction conditions: 1-octene =  $0.85 \text{ kmol/m}^3_{\text{org}}$ ;  $\text{Rh}(\text{CO})_2(\text{acac}) = 3.86 \times 10^{-3} \text{ kmol/m}^3_{\text{IL}}$ ; sulfoxantphos:Rh ratio = 5:1 ( $P:\text{Rh}$  ratio = 10:1); temperature = 393 K;  $P_{\text{CO}} = 20.7 \text{ bar}$ ,  $P_{\text{H}_2} = 20.7 \text{ bar}$ ; reaction time: 6 h; and total liquid volume:  $2.5 \times 10^{-5} \text{ m}^3$ .

oxygen from the reactor. The fresh reaction was carried out as usual. In this way, two recycle experiments were performed. The results are presented in Fig. 2. The catalyst activity and the high  $n$ :iso ratio were retained during recycle experiments indicating no important leaching of rhodium to the organic phase, as well as retention of the active complex during the experiments. The TOF of about  $40 \text{ mol}_{\text{aldehyde}}/\text{mol}_{\text{Rh}}/\text{h}$  obtained here lies within the range of published values for the homogeneous reaction with different solvents and ligands: from 25 to  $2000 \text{ mol}_{\text{aldehyde}}/\text{mol}_{\text{Rh}}/\text{h}$  (Deshpande and Chaudhari, 1988; Deshpande et al., 1992, 1993; Bronger et al., 2004a; Rosales et al., 2008; Zuidema et al., 2008).

In order to ascertain that rhodium did not leach to the organic phase, one complementary experiment was carried out using an organic phase after the reaction without the ionic liquid phase containing rhodium. In this experiment, no product formation was observed, confirming that the rhodium did not leach to the organic phase during the experiment. Thus, hydroformylation reaction takes place only in the ionic liquid phase and initial rates calculated will truly represent biphasic catalysis.

After confirmation of material balance and true biphasic catalysis, work on the kinetic investigation was undertaken. In order to study the kinetics, it is important to ensure that reactions are carried out under the kinetic regime. The experiments at different agitation speeds showed that the rate of the reaction was independent of the agitation speed beyond 1000 rpm, indicating the kinetic regime. All the reactions were therefore carried out at an agitation speed of 1200 rpm (20 Hz) to ensure the kinetic regime.

### 3.3. Kinetic study of hydroformylation of 1-octene

There are no reports on the kinetics of olefin hydroformylation using  $[\text{BuPy}][\text{BF}_4]$  ionic liquid in a biphasic medium. The kinetic studies provide valuable information for understanding the mechanism of the reaction, as well as for the reactor design. This investigation was conducted under the following standard conditions: organic phase (15 ml) consisting of heptane and olefin with a concentration of  $0.85 \text{ kmol/m}^3_{\text{org}}$ ,  $[\text{BuPy}][\text{BF}_4]$  (10 ml) with a catalyst concentration of  $1.93 \times 10^{-3} \text{ kmol/m}^3_{\text{IL}}$  and  $P:\text{Rh}$  = 10:1,  $P_{\text{H}_2} = P_{\text{CO}} = 20.7 \text{ bar}$ , temperature in the range 353–373 K and an agitation speed of 1200 rpm. The effect of catalyst concentration, 1-octene concentration, partial pressures of CO and  $\text{H}_2$  was then studied in the given range of conditions shown in Table 3. The initial rates of hydroformylation were calculated from the  $n$ -nonanal and iso-aldehydes formed during

**Table 3**

Range of conditions for the kinetic study.

Parameter, units	Range
Concentration of catalyst $[\text{Rh}(\text{CO})_2(\text{acac})]$ , $\text{kmol/m}^3_{\text{IL}}$	$(1.93\text{--}7.72) \times 10^{-3}$
Concentration of 1-octene, $\text{kmol/m}^3_{\text{org}}$	0.425–1.274
Partial pressure of hydrogen, bar	6.9–34.5
Partial pressure of carbon monoxide, bar	1.7–34.5
Temperature, K	353–373
IL liquid fraction	0.4
Agitation speed, Hz	20
Total liquid volume, $\text{m}^3$	$2.5 \times 10^{-5}$

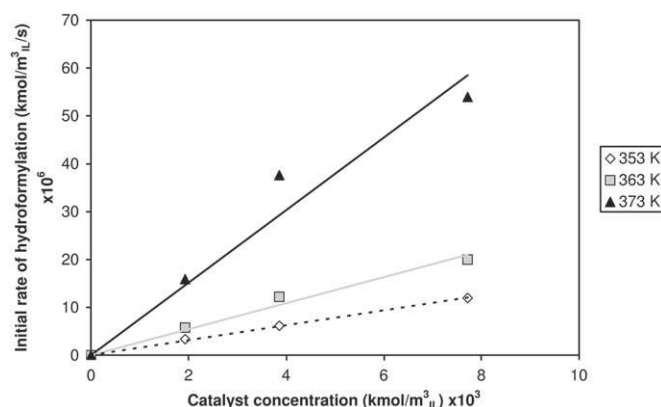


**Fig. 3.** Effect of catalyst concentration on the rate of hydroformylation. Reaction conditions: 1-octene =  $0.85 \text{ kmol/m}^3_{\text{org}}$ ;  $P:\text{Rh}$  ratio = 10:1;  $P_{\text{CO}} = 20.7 \text{ bar}$ ,  $P_{\text{H}_2} = 20.7 \text{ bar}$ ; and total liquid volume:  $2.5 \times 10^{-5} \text{ m}^3$ .

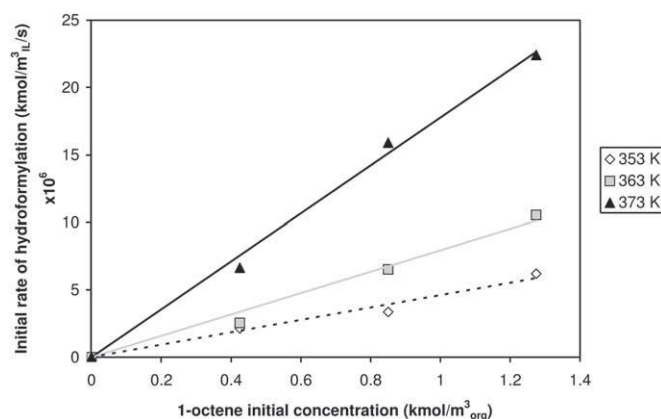


**Fig. 4.** Effect of 1-octene initial concentration on the rate of hydroformylation. Reaction conditions:  $\text{Rh}(\text{CO})_2(\text{acac}) = 1.93 \times 10^{-3} \text{ kmol/m}^3_{\text{IL}}$ ;  $P:\text{Rh}$  ratio = 10:1;  $P_{\text{CO}} = 20.7 \text{ bar}$ ,  $P_{\text{H}_2} = 20.7 \text{ bar}$ ; and total liquid volume:  $2.5 \times 10^{-5} \text{ m}^3$ .

the reaction. They were then corrected for the amount of aldehyde solubilised in the IL phase at equilibrium and expressed in a convenient unit by dividing them by the catalyst phase volume (10 ml). For this purpose, several liquid samples were withdrawn during the initial reaction period and analyzed for the product formation. As explained above, they were essentially initial rates of hydroformylation reaction calculated under low conversion of 1-octene (usually < 10–15% conversion).

The effect of catalyst concentration, partial pressures of  $\text{H}_2$  and CO, and 1-octene concentration on the initial rate of hydroformylation is shown in Figs. 3–6, respectively. The proposed mechanism for hydroformylation using sulfoxantphos as a ligand in a biphasic medium is presented in Fig. 7 (Silva et al., 2003; Pagar, 2007).

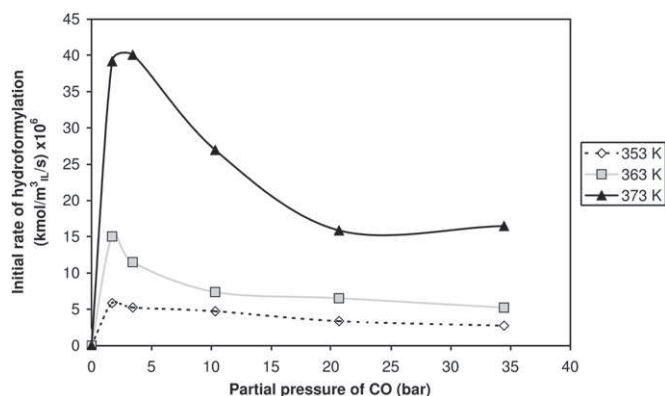


**Fig. 5.** Effect of CO partial pressure on the rate of hydroformylation. Reaction conditions: 1-octene = 0.85 kmol/m<sup>3</sup><sub>org</sub>; Rh(CO)<sub>2</sub>(acac) = 1.93 × 10<sup>-3</sup> kmol/m<sup>3</sup><sub>liq</sub>; P:Rh ratio = 10:1; P<sub>H2</sub> = 20.7 bar; and total liquid volume = 2.5 × 10<sup>-5</sup> m<sup>3</sup>.

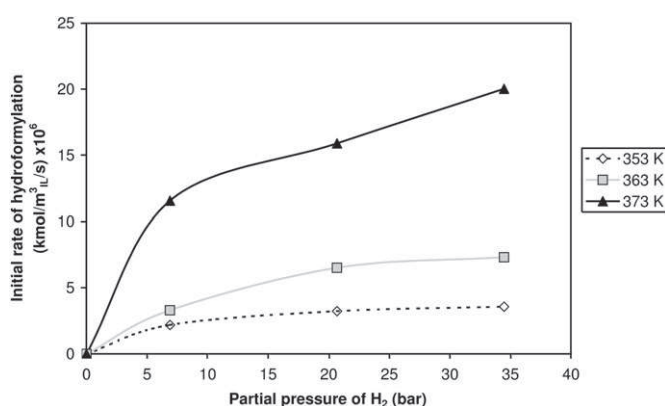


**Fig. 6.** Effect of H<sub>2</sub> partial pressure on the rate of hydroformylation. Reaction conditions: 1-octene = 0.85 kmol/m<sup>3</sup><sub>org</sub>; Rh(CO)<sub>2</sub>(acac) = 1.93 × 10<sup>-3</sup> kmol/m<sup>3</sup><sub>liq</sub>; P:Rh ratio = 10:1; P<sub>CO</sub> = 20.7 bar; and total liquid volume: 2.5 × 10<sup>-5</sup> m<sup>3</sup>.

It may be noted that the mechanism proposed is based on the in-situ IR and NMR characterization work done by the group of van Leeuwen (Goedheijt et al., 1998; Sandee et al., 1999; Silva et al., 2003; Bronger et al., 2004b). They have clearly shown that Rh(CO)<sub>2</sub>(acac) reacts with sulfoxantphos ligand in the presence of CO and H<sub>2</sub> to give principally species 1a and 1b as shown in the mechanism and predominant species present is 1a. The formation of dimeric complex, which is known to lower the activity of the rhodium catalyst can be prevented by using high H<sub>2</sub> partial pressure and low catalyst concentration, shifting the equilibrium presented in Fig. 7b almost completely to the monomeric species (Bronger et al., 2004b). Interaction of olefin with 1a leads to an olefin coordinated species 2, which is converted to alkyl species 3a and 3b, with a predominance of species 3a, due to the steric effect. Further steps are similar to the conventional mechanism proposed by Evans et al. (1968) for hydroformylation using monophosphines.

### 3.3.1. Effect of catalyst concentration

The effect of the concentration of the catalyst precursor Rh(CO)<sub>2</sub>(acac) (with the P:Rh ratio constant at 10:1) was investigated at the three temperatures by keeping the partial pressures of H<sub>2</sub> and CO constant at 20.7 bar and 1-octene concentration of 0.85 kmol/m<sup>3</sup><sub>org</sub> (Fig. 3). It was observed that the rate of the reaction increased with an increase in the catalyst concentration with a first order dependence. This type of behavior is expected since an increase in the catalyst concentration will enhance the concentration of active catalytic species and the rate of the reaction. It proves that all rhodium atoms

are working as catalyst at the same TOF whatever the catalyst loading and that no mass transfer limitation is occurring. This also indicates that Rh dimeric species might be negligible.

### 3.3.2. Effect of 1-octene concentration

The initial concentration of 1-octene was varied from 0.425 to 1.274 kmol/m<sup>3</sup><sub>org</sub> (decreasing the weight percentage of heptane in the organic mixture accordingly), while keeping the other parameters the same. The results are presented in Fig. 4. The rate was found to increase with an increase in 1-octene concentration with a first order dependence. 1-octene is not a strongly coordinating olefin and hence higher concentrations in the catalyst phase will be necessary to convert the Rh complex into an olefin coordinated complex (species 2) as shown in the proposed mechanism in Fig. 7a. Thus, an increase in 1-octene concentration in the organic phase will increase its concentration in [BuPy][BF<sub>4</sub>], leading to an enhancement in rate.

### 3.3.3. Effect of CO and H<sub>2</sub> partial pressures

To study the effect of the partial pressures of the gas, the ballast was filled up with the desired ratio of CO:H<sub>2</sub>, so that to feed the reactor up to the required total pressure with that gas composition. The ballast was then emptied and filled up with the equimolar mixture of CO/H<sub>2</sub> to maintain the desired ratio in the reactor throughout the reaction. While studying the effect of the partial pressure of a given gas, the partial pressure of the other was kept constant at 20.7 bar. Other operating parameters corresponded to standard conditions.

**3.3.3.1. Partial pressure of CO.** The rate showed a complex dependence with partial pressure of CO, as seen in Fig. 5: it first increased steeply, and then decreased with further increase in CO pressure, exhibiting a clear maximum at 2–4 bar. This inhibition of the rate with an increase in the partial pressure of CO is very typical of hydroformylation reactions, observed for both homogeneous and biphasic systems catalyzed by the rhodium complex with PPh<sub>3</sub> or TPPTS as ligands (Deshpande and Chaudhari, 1988; Deshpande et al., 1996). It is due to the side reactions leading to the formation of inactive dicarbonyl rhodium species (Fig. 7a, species 6). With an increase in CO pressure, the concentration of this species increases in the catalyst phase, reducing the concentration of the active species and hence the rate of reaction.

**3.3.3.2. Partial pressure of H<sub>2</sub>.** The rate was positively dependent on the partial pressure of H<sub>2</sub>, as shown in Fig. 6. No hydrogenation products were observed in the range of conditions studied.

As mentioned above, equilibrium of the Rh active complex with dimeric Rh species (Fig. 7b) is not likely as the increase in H<sub>2</sub> partial pressure (keeping CO pressure constant) did not considerably modify the initial rate of hydroformylation at high values. Similarly, Silva et al. (2003) observed only a marginal influence of hydrogen partial pressure on the hydroformylation of 1-octene using [(HRh(CO)<sub>2</sub>(sulfoxantphos))] in [Bmim][PF<sub>6</sub>]. High pressure NMR analysis confirmed the presence of monomeric Rh complex [(HRh(CO)<sub>2</sub>(sulfoxantphos))] with very little dimeric species.

Here, the observed increase of reaction rate with H<sub>2</sub> pressure can be explained due to an oxidative addition of hydrogen to the acyl complex to give the dihydrogen complex (Fig. 7a, species 7). However, the partial order dependence suggests that this step might not be limiting.

### 3.4. Modeling of initial reaction rates

The kinetic data observed were used for the development of a rate model. A variety of empirical models (models 1–7) and models

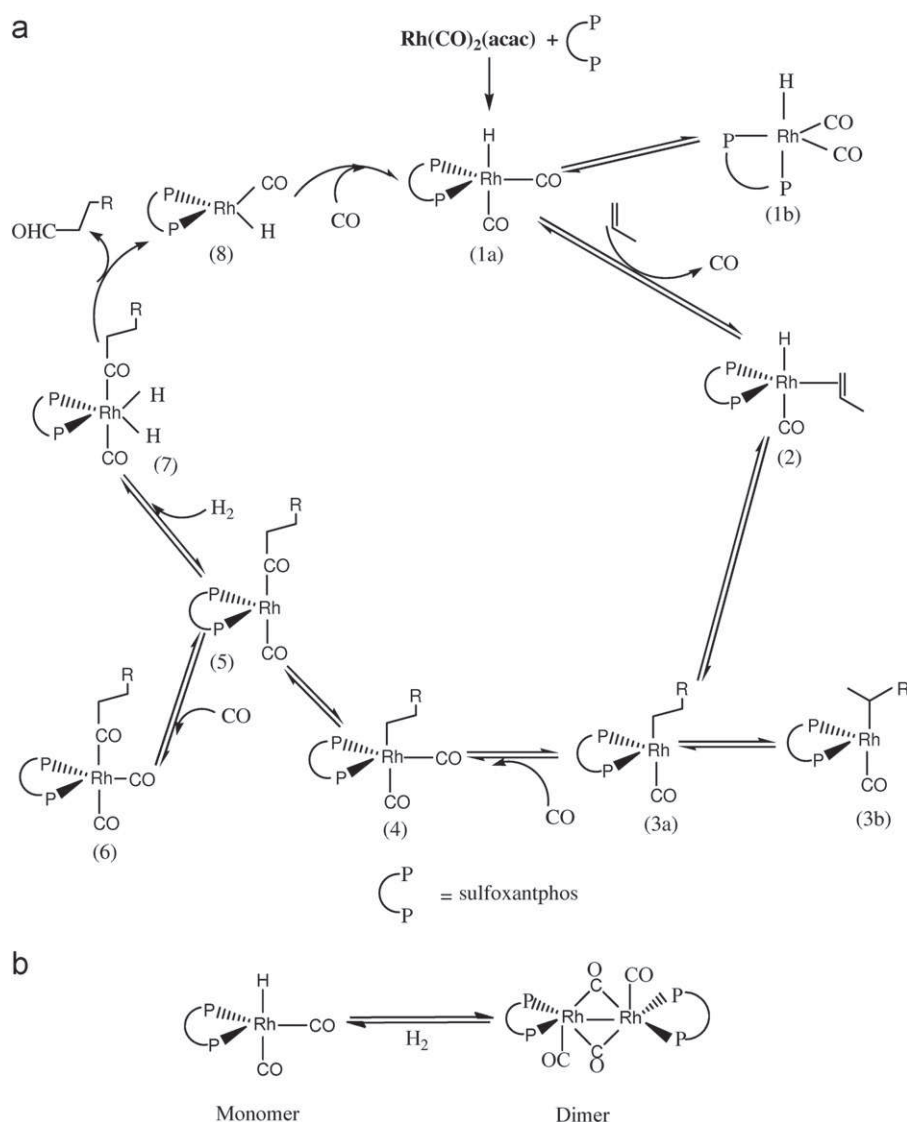


**Fig. 7.** (a) Mechanism of hydroformylation of olefins using diphosphine ligand and (b) equilibrium between Rh dimer and monomer complex.

derived from the mechanism of hydroformylation reaction (models 8–10) were evaluated for fitting the initial rate data (see Table 4). These models were selected based on the trends observed for the dependence of the rate on the different parameters. All the empirical rate models (except model 5) describe the inhibition by CO pressure; models 3 to 5 add the non-linear effect of H<sub>2</sub> pressure, while model 7 also accounts for a possible non-linear effect of an octene concentration. In models 3–4 and 7, the influence of each parameter is described in separate terms.

Mechanistic models were obtained based on the “Christiansen matrix” approach (Helfferich, 2004; Murzin and Salmi, 2005), neglecting 1b, 3b and Rh dimer species. Model 8 assumes that all the elementary steps are irreversible, while models 9 and 10 consider that only the release of aldehyde product is an irreversible step. To reduce the complexity of the system, the respective additions of CO, olefin and H<sub>2</sub> were examined as possible rate determining step, but only in the later case, the rate expression derived was found to depend upon on all the operating parameters (model 9). Finally, the expression with no limiting step is given as model 10.

The concentrations of dissolved CO, H<sub>2</sub> and 1-octene in [BuPy][BF<sub>4</sub>] required in the kinetic modeling were evaluated from

**Table 4**

Models investigated for kinetics of 1-octene hydroformylation.

Model 1: $R = \frac{kABCD}{(1 + K_b B)^2}$	Model 6: $R = \frac{kABCD}{(1 + K_a A + K_b B)^2}$
Model 2: $R = \frac{kABCD}{(1 + K_b B)^3}$	Model 7: $R = \frac{kABCD}{(1 + K_a A)(1 + K_b B)^2(1 + K_d D)}$
Model 3: $R = \frac{kABCD}{(1 + K_a A)(1 + K_b B)^2}$	Model 8: $R = \frac{kABCD}{(K_a AB + K_b AD + K_c BD + K_d ABD + K_e DB^2)}$
Model 4: $R = \frac{kABCD}{(1 + K_a A)(1 + K_b B)^3}$	Model 9: $R = \frac{kABCD}{(1 + K_a B + K_b D + K_c BD + K_d DB^2)}$
Model 5: $R = \frac{kABCD}{(1 + K_a A + K_b B)}$	Model 10: $R = \frac{kABCD}{(1 + K_a AB + K_b AD + K_c BD + K_d ABD + K_e DB^2 + K_f A + K_g AB^2 + K_h B + K_i D)}$

A, B, C and D refer to the concentrations of, respectively, dissolved H<sub>2</sub>, CO, catalyst and olefin in the IL phase.

the solubility data reported in Section 3.1. Optimization of all the models was done using the Auto2Fit software, which allows the use of about ten different numerical methods for data regression. Thus, a systematic procedure was adopted to check for the



parameter identifiability (the different algorithms must not converge to disparate sets of parameters, while displaying rather similar criteria) and to give more chance for a global minimum to be found. When required, constraint of positive value was imposed to parameters in the fitting.

The criterion for selecting the best model was based on the sum of square error (SSE) between the calculated and experimental rates

$$SSE = \sum_{i=1}^n (10^6 R_{0, \text{calc}, i} - 10^6 R_{0, \text{exp}, i})^2$$

(initial rates  $R_0$  given in kmol/m<sup>3</sup>/s).

For models 5, 6, 8, 9 and 10, the numerical methods giving the lowest criteria converged to either very high or very low values for some of the fitted parameters. Those parameters were found to largely depend on the optimization methods despite similar criteria. So the models were simplified by reducing their number of parameters according to those trends, resulting in models 5b, 6b, 8b, 9b and 10b given in Table 5. It was checked that these

derived models gave the same fitting as original model (equivalent SSE), but with more reliable parameters (as found the same whatever numerical method).

Finally regarding model 7, it was found that  $K_d$  should be very close to zero, so that this model finally became one with model 3.

Then, all selected models were evaluated using the DataFit software, in order to get confidence intervals of the parameters. Final optimization results are given in Table 5.

From these statistical data, following conclusions could be drawn:

- Model 5b was readily discarded as it did not predict the influence of CO concentration well and gave, thus, the highest SSE criteria.
- Including the non-linear dependence of the reaction rate on the H<sub>2</sub> concentration (model 3 versus model 1, model 4 versus model 2) improved the data fitting, but led to too large confidence intervals for  $K_a$  and  $k$ . Models 3 and 4 were thus not considered.
- Regarding mechanistic models, model 9 (with H<sub>2</sub> insertion as the limiting step) gave, as expected, a higher SSE than the

**Table 5**

Rate equations derived from models given in Table 4, with fitted parameters, 95% confidence intervals and SSE criteria.

Model	Temperature	$K_a$	$K_b$ (or $K$ )	$k$ (or $k'$ )	SSE
1: $R = \frac{kABCD}{(1+K_bB)^2}$	$T=353\text{ K}$	—	123.8 ( ± 35.3)	7293 ( ± 3268)	8.51
	$T=363\text{ K}$	—	188.6 ( ± 50.4) m <sub>IL</sub> <sup>3</sup> /kmol	28208 ( ± 12017) (m <sub>IL</sub> <sup>3</sup> /kmol) <sup>3</sup> /s	31.44
	$T=373\text{ K}$	—	208.1 ( ± 51.7)	106159 ( ± 42017)	216.67
2: $R = \frac{kABCD}{(1+K_bB)^3}$	$T=353\text{ K}$	—	45.82 ( ± 9.67)	4848 ( ± 1885)	10.83
	$T=363\text{ K}$	—	59.86 ( ± 12.40) m <sub>IL</sub> <sup>3</sup> /kmol	15487 ( ± 6000) (m <sub>IL</sub> <sup>3</sup> /kmol) <sup>3</sup> /s	53.50
	$T=373\text{ K}$	—	66.44 ( ± 10.38)	60014 ( ± 17486)	266.97
3: $R = \frac{kABCD}{(1+K_aA)(1+K_bB)^2}$	$T=353\text{ K}$	79.28 ( ± 188.2)	119.9 ( ± 26.2)	30017 ( ± 55429)	4.55
	$T=363\text{ K}$	27.76 ( ± 88.04) m <sub>IL</sub> <sup>3</sup> /kmol	183.8 ( ± 47.7) m <sub>IL</sub> <sup>3</sup> /kmol	54275 ( ± 87007) (m <sub>IL</sub> <sup>3</sup> /kmol) <sup>3</sup> /s	26.92
	$T=373\text{ K}$	91.09 ( ± 258.9)	202.3 ( ± 45.2)	371649 ( ± 774001)	161.09
4: $R = \frac{kABCD}{(1+K_aA)(1+K_bB)^3}$	$T=353\text{ K}$	79.45 ( ± 234.2)	44.81 ( ± 8.02)	20177 ( ± 45938)	6.94
	$T=363\text{ K}$	26.49 ( ± 115.2) m <sub>IL</sub> <sup>3</sup> /kmol	58.90 ( ± 12.43) m <sub>IL</sub> <sup>3</sup> /kmol	29464 ( ± 62505) (m <sub>IL</sub> <sup>3</sup> /kmol) <sup>3</sup> /s	49.33
	$T=373\text{ K}$	90.50 ( ± 304.4)	65.28 ( ± 9.73)	211856 ( ± 517028)	217.57
5b: $R = k'ACD$	$T=353\text{ K}$	—	—	$k' = 7.99$ ( ± 1.17)	21.18
	$T=363\text{ K}$	—	—	$k' = 16.00$ ( ± 3.32) (m <sub>IL</sub> <sup>3</sup> /kmol) <sup>2</sup> /s	142.80
	$T=373\text{ K}$	—	—	$k' = 51.68$ ( ± 12.34)	1447.18
6b: $R = \frac{k'ABCD}{(A+KB)^2}$	$T=353\text{ K}$	—	$K = 4.85$ ( ± 1.15)	$k' = 11.56$ ( ± 4.29)	5.87
	$T=363\text{ K}$	—	$K = 6.49$ ( ± 1.64) (—)	$k' = 33.98$ ( ± 13.63) (m <sub>IL</sub> <sup>3</sup> /kmol)/s	28.07
	$T=373\text{ K}$	—	$K = 5.82$ ( ± 1.34)	$k' = 84.48$ ( ± 30.88)	186.12
7: $R = \frac{kABCD}{(1+K_aA)(1+K_bB)^2(1+K_dD)}$			became one with Model 3 ( $K_d \neq 0$ )		—
					—
					—
8b: $R = \frac{k'ACD}{(A+KBD)}$	$T=353\text{ K}$	—	$K = 138.5$ ( ± 86.9)	$k' = 0.58$ ( ± 0.15)	7.08
	$T=363\text{ K}$	—	$K = 264.7$ ( ± 131.6) m <sub>IL</sub> <sup>3</sup> /kmol	$k' = 1.49$ ( ± 0.41) (m <sub>IL</sub> <sup>3</sup> /kmol)/s	34.92
	$T=373\text{ K}$	—	$K = 249.2$ ( ± 112.5)	$k' = 4.34$ ( ± 1.13)	255.61
9b: $R = \frac{k'ACD}{(1+KDB)}$	$T=353\text{ K}$	—	$K = 3885$ ( ± 2903)	$k' = 14.77$ ( ± 4.85)	10.99
	$T=363\text{ K}$	—	$K = 7952$ ( ± 4162) (m <sub>IL</sub> <sup>3</sup> /kmol) <sup>2</sup>	$k' = 43.10$ ( ± 12.78) (m <sub>IL</sub> <sup>3</sup> /kmol) <sup>2</sup> /s	39.97
	$T=373\text{ K}$	—	$K = 9196$ ( ± 4431)	$k' = 154.7$ ( ± 43.8)	299.85
10b: $R = \frac{k'ACD}{(1+KAB)}$	$T=353\text{ K}$	—	$K = 554.1$ ( ± 229.2)	$k' = 15.74$ ( ± 3.01)	4.07
	$T=363\text{ K}$	—	$K = 1252$ ( ± 445) (m <sub>IL</sub> <sup>3</sup> /kmol) <sup>2</sup>	$k' = 43.84$ ( ± 8.84) (m <sub>IL</sub> <sup>3</sup> /kmol) <sup>2</sup> /s	19.18
	$T=373\text{ K}$	—	$K = 1865$ ( ± 699)	$k' = 156.4$ ( ± 34.4)	186.60

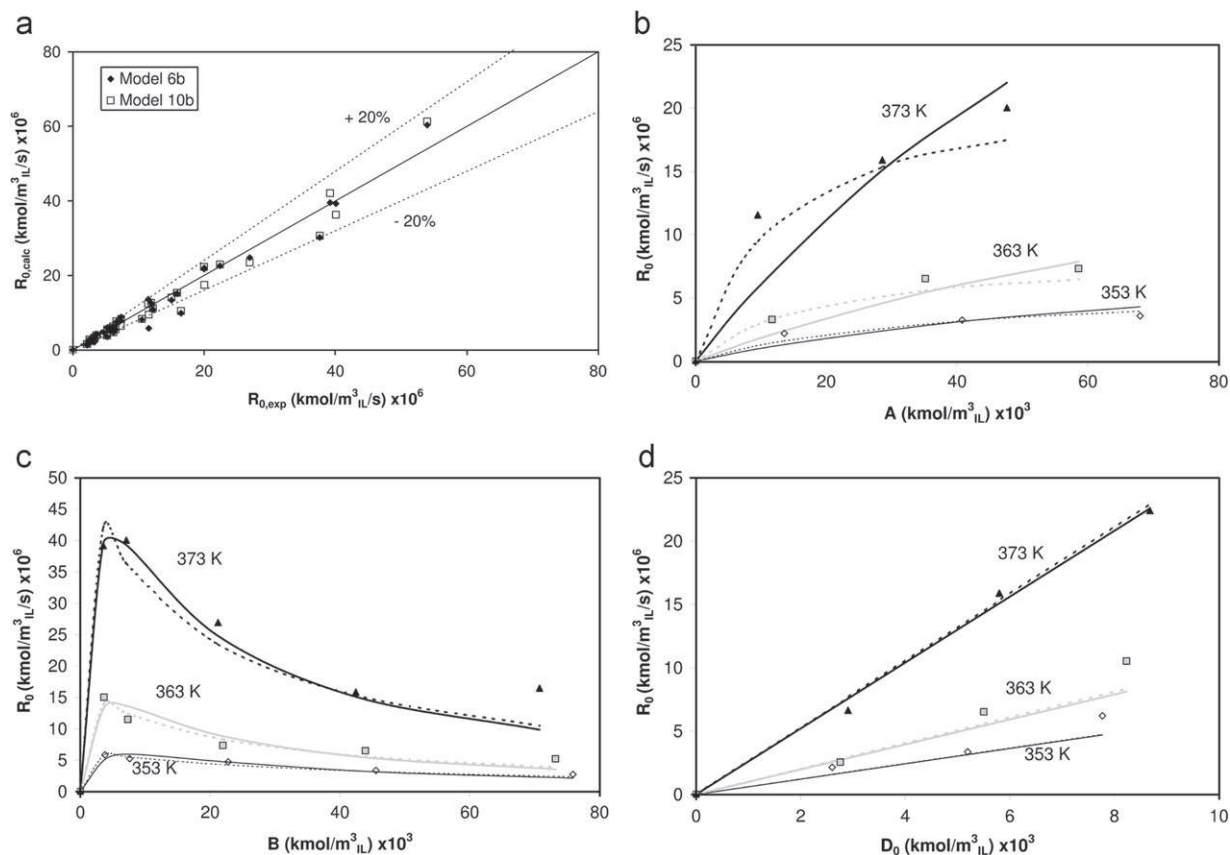


**Fig. 8.** Comparison of experimental data and model 6b and 10b calculations: (a) parity plots, (b) effect of  $H_2$  concentration in the IL phase, (c) effect of CO concentration in the IL phase, (d) effect of the initial concentration of 1-octene in the IL phase. Fig. b–d: dots are experimental data, continuous line predictions of model 6b, and dashed line predictions of model 10b.

more complex model 10, as the hydroformylation rate exhibited a marked non-linear trend with respect to the  $H_2$  partial pressure. Model 8, which shows CO inhibition and partial order for both  $H_2$  and olefin, led to an intermediate criteria.

- Finally, model 6b (empirical) and model 10b derived from the mechanistic model 10 appeared to be the best ones to represent the kinetic data, providing low SSE and reasonable confidence intervals. Parity plot for those two models is given in Fig. 8a. The effects of operating parameters and corresponding model calculations are also shown in Fig. 8b–d. Both models accurately predict first order dependence with respect to catalyst and 1-olefin concentrations, non-linearity of  $H_2$  pressure effect and CO inhibition.

Arrhenius plot of parameter  $k'$  led to an “apparent” activation energy in the range 26–30 kcal/mol depending on the model. Accounting for the confidence interval, parameter  $K$  was not found to depend much on temperature in model 6b, but it clearly increased with temperature in model 10b. In the later case, plot of  $\ln(K)$  versus  $1/T$  gave an almost linear trend (equivalent energy of 15.9 kcal/mol).

#### 4. Conclusions

The kinetics of hydroformylation of 1-octene using [BuPy][BF<sub>4</sub>]/heptane biphasic system and Rh(CO)<sub>2</sub>(acac)/sulfoxanthphos catalyst system was investigated. The concentrations of dissolved CO,  $H_2$  and 1-octene in [BuPy][BF<sub>4</sub>] required in the modeling were evaluated from solubility data obtained experimentally at different temperatures.

The hydroformylation rate was found to be the first order with respect to catalyst and 1-octene concentrations and fractional order with respect to the hydrogen partial pressure. Its evolution versus CO concentration exhibited a maximum, indicating an inhibition at higher pressures. Based on these data, two rate equations (one empirical and one derived from the reaction mechanism) were proposed that accurately fit the initial rate data, after an examination of several empirical models and a rigorous model discrimination procedure.

#### List of notations and symbols

$A$	concentration of $H_2$ in IL phase, $\text{kmol}/\text{m}^3_{\text{IL}}$
$B$	concentration of CO in IL phase, $\text{kmol}/\text{m}^3_{\text{IL}}$
$C$	concentration of catalyst in IL phase, $\text{kmol}/\text{m}^3_{\text{IL}}$
$D$	concentration of 1-octene in IL phase, $\text{kmol}/\text{m}^3_{\text{IL}}$
$H$	Henry's law constant, $\text{bar m}^3_{\text{IL}}/\text{kmol}$
$k$	reaction rate constant as defined by models 1–10 (Table 4), $(\text{m}^3_{\text{IL}}/\text{kmol})^3/\text{s}$
$K_a, K_b, K_c, K_d$	equilibrium constants as defined by models 1–10 (Table 4), $\text{m}^3_{\text{IL}}/\text{kmol}$ or $(\text{m}^3_{\text{IL}}/\text{kmol})^2$ or $(\text{m}^3_{\text{IL}}/\text{kmol})^3$
$K_{w,non}$	partition coefficient of $n$ -nonanal between the IL phase and the organic phases at considered equilibrium, %wt in IL phase/%wt in org. phase
$K_{w,oct}$	partition coefficient of 1-octene between the IL and the organic phases at considered equilibrium, %wt in IL phase/%wt in org. phase
$R$	rate of hydroformylation, $\text{kmol}/\text{m}^3_{\text{IL}}/\text{s}$
$T$	temperature, $K$

## Subscripts

IL ionic liquid phase  
org organic phase  
0 at initial time

## Acknowledgement

IFCPAR, under the project 3305-2, is gratefully acknowledged for the financial support.

## References

- Arnoldy, P., 2000. Chapter 8: process aspects of rhodium-catalyzed hydroformylation. In: van, P.W.N.M., Leeuwen, Claver, C. (Eds.), *Rhodium Catalyzed Hydroformylation*. Kluwer Academic Publishers, pp. 203–231.
- Beller, M., Cornils, B., Frohning, C.D., Kohlpaintner, C.W., 1995. Progress in hydroformylation and carbonylation. *J. Mol. Catal. A* 104, 17–85.
- Brasse, C.C., Englert, U., Salzer, A., Waffenschmidt, H., Wasserscheid, P., 2000. Ionic phosphine ligands with cobaltocenium backbone: novel ligands for the highly selective, biphasic, rhodium-catalyzed hydroformylation of 1-octene in ionic liquids. *Organometallics* 19, 3818–3823.
- Brauer, D.J., Kottsieper, K.W., Liek, C., Stelzer, O., Waffenschmidt, H., Wasserscheid, P., 2001. Phosphines with 2-imidazolium and para-phenyl-2-imidazolium moieties—synthesis and application in two-phase catalysis. *J. Organomet. Chem.* 630, 177–184.
- Bronger, R.P.J., Bermon, J.P., Herwig, J., Kamer, P.C.J., van Leeuwen, P.W.N.M., 2004a. Phenoxaphosphino-modified xantphos-type ligands in the rhodium-catalysed hydroformylation of internal and terminal alkenes. *Adv. Synth. Catal.* 346 (789–799).
- Bronger, R.P.J., Silva, S.M., Kamer, P.C.J., van Leeuwen, P.W.N.M., 2004b. A novel dicationic phenoxaphosphino-modified xantphos-type ligand: hydroformylation in ionic liquids. *Dalton Trans.* 10 (1590–1596).
- Chauvin, Y., Olivier-Bourbigou, H., 1995. Non-aqueous ionic liquids as reaction solvents. *Chemtech* 25, 26–30.
- Chauvin, Y., Musmann, L., Olivier, H., 1995. A novel class of versatile solvents for two-phase catalysis: hydrogenation, isomerization, and hydroformylation of alkenes catalyzed by rhodium complexes in liquid 1, 3-dialkylimidazolium salts. *Angew. Chem. Int. Ed.* 34, 2698–2700.
- Deng, C., Ou, G., She, J., Yuan, Y., 2007. Biphasic asymmetric hydroformylation and hydrogenation by water-soluble rhodium and ruthenium complexes of sulfonated (R)-2,2'-bis(diphenylphosphino)-1,1'-binaphthyl in ionic liquids. *J. Mol. Catal. A* 270, 76–82.
- Deshpande, R.M., Chaudhari, R.V., 1988. Kinetics of hydroformylation of 1-hexene using  $\text{HRh}(\text{CO})(\text{PPh}_3)_3$  complex catalyst. *Ind. Eng. Chem. Res.* 27, 1996–2002.
- Deshpande, R.M., Divekar, S.S., Bhanage, B.M., Chaudhari, R.V., 1992. Effect of solvent on the kinetics of hydroformylation of 1-hexene using  $\text{HRh}(\text{CO})(\text{PPh}_3)_3$  catalyst. *J. Mol. Catal.* 77, L13–L17.
- Deshpande, R.M., Bhanage, B.M., Divekar, S.S., Chaudhari, R.V., 1993. Solvent effects in hydroformylation of 1-octene using  $\text{HRh}(\text{CO})(\text{PPh}_3)_3$ : effect of  $\text{PPh}_3$  addition on the rate of reaction. *J. Mol. Catal.* 78, L37–L40.
- Deshpande, R.M., Purwanto, Delmas, H., Chaudhari, R.V., 1996. Kinetics of hydroformylation of 1-octene using  $[\text{Rh}(\text{COD})\text{Cl}]_2\text{-TPPTS}$  complex catalyst in a two-phase system in the presence of a cosolvent. *Ind. Eng. Chem. Res.* 35, 3927–3933.
- Dupont, J., Silva, S.M., de Souza, R.F., 2001. Mobile phase effects in Rh/sulfonated phosphine/molten salts catalysed the biphasic hydroformylation of heavy olefins. *Catal. Lett.* 77, 131–133.
- Evans, D., Osborne, J., Wilkinson, G., 1968. Hydroformylation of alkenes by use of rhodium complex catalysts. *J. Chem. Soc. A*, 3133–3142.
- Favre, F., Olivier-Bourbigou, H., Commereuc, D., Saussine, L., 2001. Hydroformylation of 1-hexene with rhodium in non-aqueous ionic liquids: how to design the solvent and the ligand to the reaction. *Chem. Commun.*, 1360–1361.
- Goedheijt, M.S., Kamer, P.C.J., van Leeuwen, P.W.N.M., 1998. A water-soluble diphosphine ligand with a large 'natural' bite angle for two-phase hydroformylation of alkenes. *J. Mol. Catal. A* 134, 243–249.
- Haumann, M., Riisager, A., 2008. Hydroformylation in room temperature ionic liquids (RTILs): catalyst and process developments. *Chem. Rev.* 108, 1474–1497.
- Heffferich, F.G., 2004. Kinetics of Multistep Reactions, *Comprehensive Chemical Kinetics* second ed. Elsevier 40.
- Horvath, I.T., Rabai, J., 1994. Facile catalyst separation without water: fluorous biphasic hydroformylation of olefins. *Science* 266, 72–75.
- Horvath, I.T., Rabai, J., 1995. Fluorous multiphase systems. *US Pat.* 5463082.
- Kong, F., Jiang, J., Jin, Z., 2004. Ammonium salts with polyether-tail: new ionic liquids for rhodium catalyzed two-phase hydroformylation of 1-tetradecene. *Catal. Lett.* 96, 63–65.
- Kottsieper, K.W., Stelzer, O., Wasserscheid, P., 2001. 1-Vinylimidazole—a versatile building block for the synthesis of cationic phosphines useful in ionic liquid biphasic catalysis. *J. Mol. Catal. A* 175, 285–288.
- Kuntz, E.G., 1987. Homogeneous catalysis... in water. *Chemtech* 17, 570–575.
- Mathivet, T., Monflier, E., Castanet, Y., Mortreux, A., Couturier, J.L., 2002. Hydroformylation of higher olefins by rhodium/tris-(( $^1\text{H}$ ,  $^1\text{H}$ ,  $^2\text{H}$ ,  $^2\text{H}$ -perfluorodecyl)phenyl)phosphites complexes in a fluorocarbon/hydrocarbon biphasic medium: effects of fluorinated groups on the activity and stability of the catalytic system. *Tetrahedron* 58, 3877–3888.
- Mehnert, C.P., Cook, R.A., Dispenziere, N.C., Mozeleski, E.J., 2004. Biphasic hydroformylation catalysis in ionic liquid media. *Polyhedron* 23, 2679–2688.
- Murzin, D., Salmi, T., 2005. *Catalytic Kinetics*. Elsevier Science & Technology.
- Omotowa, B.A., Shreeve, J.M., 2004. Triazine-based polyfluorinated triquaternary liquid salts: synthesis, characterization, and application as solvents in rhodium(I)-catalyzed hydroformylation of 1-octene. *Organometallics* 23, 783–791.
- Owens, G.S., Abu-Omar, M.M., 2002. Comparative kinetic investigations in ionic liquids using the MTO/peroxide system. *J. Mol. Catal. A* 187, 215–225.
- Pagar, N.S., 2007. Studies in hydroformylation reaction using homogeneous and novel heterogenized transition metal catalysts. Ph. D. Thesis, University of Pune, India.
- Peng, Q., Deng, C., Yang, Y., Dai, M., Yuan, Y., 2007. Recycle and recovery of rhodium complexes with water-soluble and amphiphilic phosphines in ionic liquids for hydroformylation of 1-hexene. *React. Kinet. Catal. Lett.* 90, 53–60.
- Rosales, M., Chacón, G., González, A., Pacheco, I., Baricelli, P.J., Melean, L.G., 2008. Kinetics and mechanisms of homogeneous catalytic reactions: part 9. Hydroformylation of 1-hexene catalyzed by a rhodium system containing a tridentate phosphine. *J. Mol. Catal. A* 287, 110–114.
- Sandee, A.J., Slagt, V.F., Reck, J.N.H., Kamer, P.C.J., Van Leeuwen, P.W.N.M., 1999. A stable and recyclable supported aqueous phase catalyst for highly selective hydroformylation of higher olefins. *Chem. Commun.*, 1633–1634.
- Sharma, A., Julcour, C., Kelkar, A.A., Deshpande, R.M., Delmas, H., 2009. Mass transfer and solubility of CO and H<sub>2</sub> in ionic liquid. Case of [Bmim][PF<sub>6</sub>] with gas-inducing stirrer reactor. *Ind. Eng. Chem. Res.* 48, 4075–4082.
- Sharma, A., Julcour-Lebigue, C., Deshpande, R.M., Kelkar, A.A., Delmas, H., 2010. Hydroformylation of 1-octene using [Bmim][PF<sub>6</sub>]-decane biphasic media and rhodium complex catalyst: thermodynamic properties and kinetic study. *Ind. Eng. Chem. Res.* 49, 10698–10706.
- Silva, S.M., Bronger, R.P.J., Freixa, Z., Dupont, J., van Leeuwen, P.W.N.M., 2003. High pressure infrared and nuclear magnetic resonance studies of the rhodium-sulfoxantphos catalysed hydroformylation of 1-octene in ionic liquids. *New J. Chem.* 27, 1294–1296.
- Varshavskii, Y.S., Cherkasova, T.G., 1967. *Russ. J. Inorg. Chem.* 12, 899.
- Wasserscheid, P., Waffenschmidt, H., Machnitzki, P., Kottsieper, K.W., Stelzer, O., 2001. Cationic phosphine ligands with phenylguanidinium modified xanthene moieties—a successful concept for highly regioselective, biphasic hydroformylation of oct-1-ene in hexafluorophosphate ionic liquids. *Chem. Commun.*, 451–452.
- Wasserscheid, P., van Hal, R., Bösmann, A., 2002. 1-*n*-Butyl-3-methylimidazolium ([Bmim]) octylsulfate—an even 'greener' ionic liquid. *Green Chem.* 4, 400–404.
- Welton, T., 1999. Room-temperature ionic liquids. *Solvents for synthesis and catalysis*. *Chem. Rev.* 99, 2071–2084.
- Zhao, D., Wu, M., Kou, Y., Min, E., 2002. Ionic liquids: applications in catalysis. *Catal. Today* 74, 157–189.
- Zuidema, E., Escorihuela, L., Eichelsheim, T., Carbó, J.J., Bo, C., Kamer, P.C.J., van Leeuwen, P.W.N.M., 2008. The rate-determining step in the rhodium-xantphos-catalyzed hydroformylation of 1-octene. *Chem. Eur. J.* 14, 1843–1853.